


RESEARCH ARTICLE

Open Access



Anti-inflammatory protein TNF α -stimulated gene-6 (TSG-6) reduces inflammatory response after brain injury in mice

Kazadi Nadine Mutoji¹, Mingxia Sun¹, Amanda Nash^{1,3}, Sudan Puri¹, Vincent Hascall² and Vivien J. Coulson-Thomas^{1*} 

Abstract

Background: Current research suggests that the glial scar surrounding penetrating brain injuries is instrumental in preserving the surrounding uninjured tissue by limiting the inflammatory response to the injury site. We recently showed that tumor necrosis factor (TNF)-stimulated gene-6 (TSG-6), a well-established anti-inflammatory molecule, is present within the glial scar. In the present study we investigated the role of TSG-6 within the glial scar using TSG-6 *null* and littermate control mice subjected to penetrating brain injuries.

Results: Our findings show that mice lacking TSG-6 present a more severe inflammatory response after injury, which was correlated with an enlarged area of astrogliosis beyond the injury site.

Conclusion: Our data provides evidence that TSG-6 has an anti-inflammatory role within the glial scar.

Keywords: TSG-6, Glial scar, Astrocytes, Glycosaminoglycans and inflammation

Background

Traumatic brain injury (TBI) is a major medical concern that affects over 10 million people in the world each year [1, 2]. A variety of injuries can cause TBI leading to a range of injury severities [3–7]. With improved medical interventions over the years, the mortality rate due to TBI has decreased, resulting in a significant number of people living with the long-term effects of TBI. It is well accepted that in addition to the immediate effects of TBI there are also multiple potential long-term gradually evolving sequelae that are influenced by the type of injury, severity of the injury and medical interventions at the time of injury [8, 9]. Additionally, a link between mild traumatic brain injuries and Alzheimer's disease or chronic traumatic encephalopathy has long been

suspected [10]. At present, long-term effects of repeated TBI have been seen in multiple sports-related injuries, including post-traumatic parkinsonism, post-traumatic dementia and chronic post-concussion syndrome [11–14]. Thus, studying the short- and long-term consequences of TBI at a cellular and molecular level may lead to a new understanding and perhaps better long-term management of such injuries via new and/or refined treatment strategies.

Astrogliosis is a hallmark of TBI, which commences hours after injury and leads to an abnormal increase in the number of activated astrocytes in and around the injury site [15, 16]. Immediately after injury (acute phase), astrocytes are activated, becoming highly proliferative and up-regulating the production of extracellular proteins [17–19]. These astrocytes and their deposited extracellular matrix in and around the injury site form a glial scar. Over the years, a significant body of evidence has demonstrated that the glial scar contains molecules,

*Correspondence: vcoulsonthomas@gmail.com; vjcoulso@central.uh.edu

¹ College of Optometry, University of Houston, 4901 Calhoun Road, Houston, TX 77204-2020, USA

Full list of author information is available at the end of the article



such as chondroitin sulfate proteoglycans (CSPGs), that impede axonal growth, thus inhibiting neuronal regeneration [15, 20–23]. The intensity of the acute and chronic reactive astrogliosis, including the quantity and composition of the glial scar, affects immediate and long-term effects of TBI [6, 16, 24, 25]. Penetrating brain injuries (PBIs) cause direct parenchymal laceration, neuronal cell loss and hemorrhage, which lead to focal tissue damage at the injury site. Astrogliosis is triggered after TBIs forming a glial scar in and around the injury site [26–29]. Importantly, uninjured tissue bordering the injury site is also subject to astrogliosis, and the process of glial scarring therefore extends beyond the injury site [30]. Given the fact that glial scarring limits regeneration after injury, many studies have investigated whether limiting astrogliosis after injury, with particular focus on limiting deposition, could potentially promote regeneration [23, 27, 31–34]. Although many studies were able to demonstrate beneficial effects of limiting glial scarring on neuronal regeneration, many others were inconclusive or actually found there was an increased inflammatory response culminating in tissue damage beyond the injury site and an increase in neuronal loss. Thus, mounting evidence indicates that reactive astrocytes surrounding the injury site are instrumental in preserving the surrounding uninjured tissue by forming scar borders, which separate damaged and inflamed tissue from adjacent viable neural tissue [15, 16, 24, 35–40]. Sofroniew and colleagues elegantly demonstrated that targeting astrocytes after brain and spinal cord injury leads to increased inflammation, delayed recovery and increased neuronal loss [39, 41–44]. Moreover, the inhibition of astrocyte proliferation prolongs the healing period following central nervous system (CNS) injury [45]. Data from Hermann et al. show that GFAP-driven ablation of STAT3 in astrocytes leads to the loss of lesion demarcation and subsequent glial scar formation, and, in turn, results in increased invasion of inflammatory cells into adjacent viable tissue and further spread of inflammation [46]. This suggests that early glial scar formation by astrocytes restricts movement of inflammatory cells located within the lesion site into adjacent healthy tissue, thereby restricting tissue damage to the injury site. Thus, a recent body of evidence suggests scar tissue bordering the injury site is necessary for limiting inflammation and tissue damage to the injury site [37, 41]. There is currently a significant number of studies investigating how reactive astrocytes regulate and limit inflammation to the injury site, and which cellular components and major pathways could play a role in this process [20, 35, 41, 45, 47].

We recently found that tumor necrosis factor (TNF)-stimulated gene-6 (TSG-6) is secreted by astrocytes after injury and is a major constituent of the glial scar, but the

role it plays within the glial scar remains to be established [48]. TSG-6 is a 35-kDa protein that is secreted by a wide range of cell types in response to inflammatory mediators and growth factors [49], and was originally identified as a gene product induced in fibroblasts by TNF [12]. TSG-6 contains a link module domain that mediates its interaction with the glycosaminoglycans (GAGs) hyaluronan (HA) and CS [49–51]. Our recent study identified that TSG-6 is expressed in the CNS, where it catalyzes the transfer of heavy chains (HCs) from Inter- α -Inhibitor ($\text{I}\alpha\text{I}$, also known as ITI) onto HA, forming a specialized HA/HC/TSG-6 matrix within the glial scar, but the role of this specialized matrix within the glial scar remains to be established [48, 52–56]. This specific HA/HC/TSG-6 matrix has previously been shown to be monocyte-adhesive in other tissues and is believed to be present in most, if not all, inflammatory processes [57, 58]. These TSG-6 modified HA matrices bind inflammatory cells, and the interaction of these cells with this matrix modulates their responses, which are central to pathological inflammation [59–65]. The main objective of this study was to investigate the role TSG-6, a constituent of the glial scar, has in astrogliosis after a PBI. Given the well-characterized anti-inflammatory role of TSG-6 in other sites, the premise of this study was that TSG-6 could participate in the formation of an immunosuppressive environment within the glial scar. Our findings show that *TSG-6 null* mice present a more severe inflammatory response and increased glial scar deposition after injury when compared to littermate control mice. This increased inflammatory response in *TSG-6 null* mice was correlated with an enlarged area of astrogliosis beyond the injury site.

Results

TSG-6 expression after PBI

In this study, transgenic *Tsg-6 null* mice (*Tnfrp6^{Δ/Δ}*), hereafter referred to as *Tsg-6^{-/-}* mice, and heterozygous mice, hereafter referred to as *Tsg-6^{+/-}* mice, were used to investigate the role of TSG-6 in the glial scar. In order to investigate whether TSG-6 is present in the glial scar after brain injury, we analyzed the expression profile of *Tsg6* in the injury site and injured hemisphere before and after a PBI in *Tsg-6^{+/-}* mice (Fig. 1A). There was a two-fold increase in *Tsg-6* expression 5 days after injury when compared to uninjured mice. There was a further increase in *Tsg-6* expression over time after injury, with expression increasing two fold from 5 to 10 days after injury (Fig. 1A). Interestingly, we did not find a difference in the expression levels of *Tsg-6* between the injury site and the remaining hemisphere, indicating that *Tsg-6* expression is not contained solely to the injury site (Fig. 1A). Therefore, there is also an increase in *Tsg-6* expression in the surrounding tissue after injury. No *Tsg-6* expression was

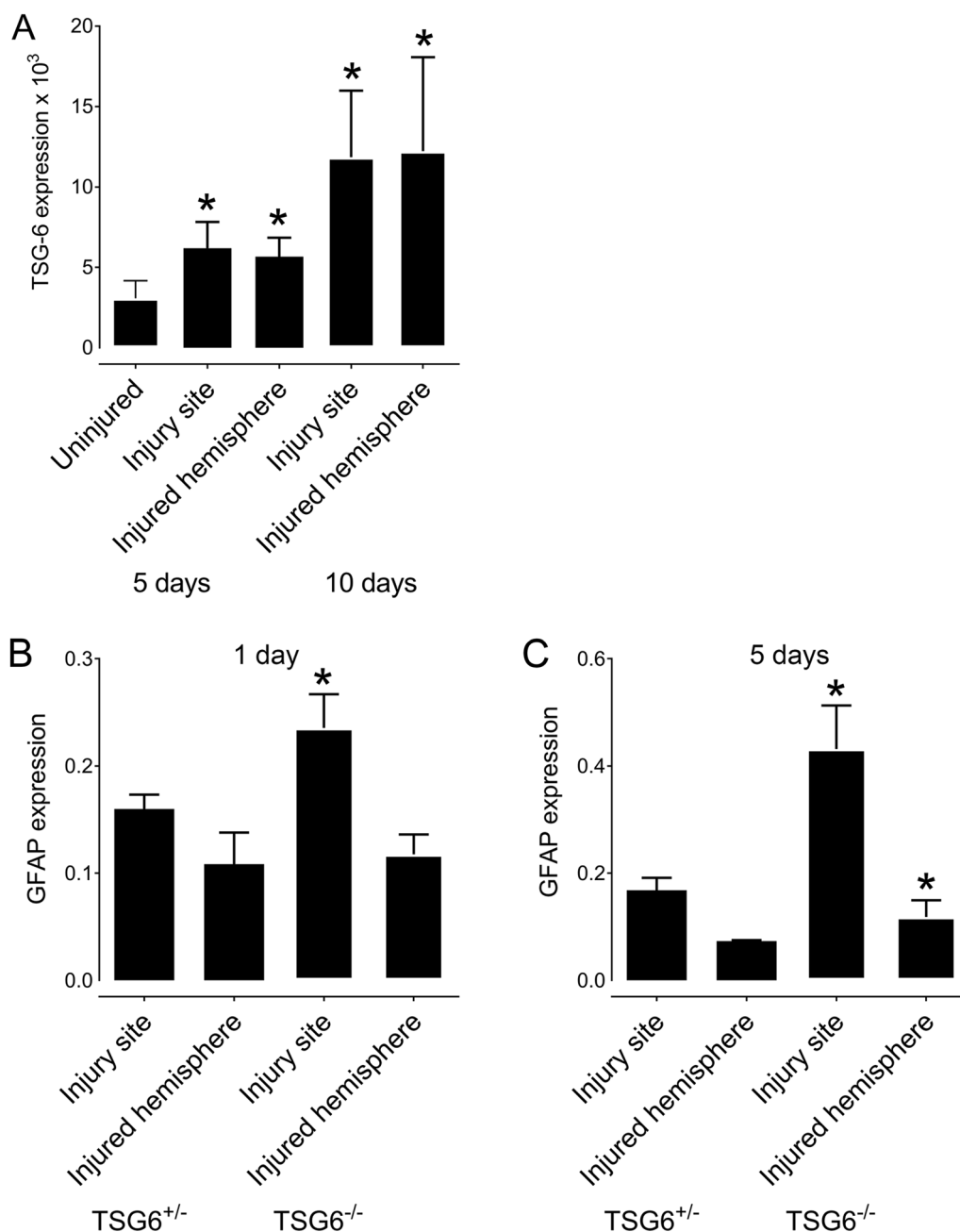


Fig. 1 TSG-6 and GFAP expression after PBI. TSG-6 and GFAP mRNA expressions were quantified in the injury site and the injured hemisphere after PBI. **A** *TSG^{+/-}* mice were subjected to PBI, and the injury site and remaining injured hemisphere were collected 5 and 10 days after injury for analysis of TSG-6 expression. **B, C** *TSG^{+/-}* and *TSG-6^{-/-}* mice were subjected to PBI, and the injury site and remaining injured hemisphere were collected 1 day (**B**) and 5 days (**C**) after injury for analysis of GFAP expression. * = $p \leq 0.05$ comparing *TSG-6^{+/-}* and *TSG-6^{-/-}* mice

identified in any of the samples from *Tsg-6^{-/-}* mice confirming that these mice are indeed *null* for *Tsg-6*.

Analysis of astrocyte recruitment after PBI

We assessed the level of astrogliosis in the injury site and in the remaining injured hemisphere by quantifying the

levels of GFAP⁺ astrocytes using real-time PCR (Fig. 1B, C). For such, we isolated mRNA from the injury site and remaining injured hemisphere 1 and 5 days after injury of *Tsg-6^{-/-}* and *Tsg-6^{+/-}* mice. Both *Tsg-6^{-/-}* and *Tsg-6^{+/-}* mice presented an increase in the levels of GFAP expression in the injury site when compared to the remaining

injured hemisphere, which corroborates literature [36, 63, 64]. *Tsg-6^{-/-}* mice showed a significant increase in GFAP levels within the injury site at both 1 and 5 days post-injury when compared to *Tsg-6^{+/-}* mice (Fig. 1B, C). This data indicates that *Tsg-6^{-/-}* mice have more astrocytes in the injury site when compared to *Tsg-6^{+/-}* mice. At 5 days after injury, there was a significant increase in GFAP expression in the injured hemisphere of *Tsg-6^{-/-}* mice compared to *Tsg-6^{+/-}* mice, indicating that *Tsg-6^{-/-}* mice present astrogliosis beyond the injury site at 5 days post-injury.

The effect of TSG-6 on the secretion of inflammatory markers after PBI

The inflammatory response was also assessed in *Tsg-6^{-/-}* and *Tsg-6^{+/-}* mice 1, 5 and 10 days post-injury by quantifying the expression levels of *NFκB*, *Rantes* and *IL1β* (Fig. 2). Higher expression levels of *NFκB*, *Rantes* and *IL1β* were detected in *Tsg-6^{-/-}* mice when compared to *Tsg-6^{+/-}* mice during the acute phase after injury. Specifically, a ~2.5-fold and threefold increase in *NfκB* expression was found in the injury site and remaining injured hemisphere, respectively, in *Tsg-6^{-/-}* mice compared to *Tsg-6^{+/-}* mice 5 days after injury (Fig. 2B). 10 days after injury there was still a significant increase in *NfκB* expression in the surrounding hemisphere of *Tsg-6^{-/-}* mice when compared to *Tsg-6^{+/-}* mice (Fig. 2C). No significant differences were found in the expression of *NfκB* between *Tsg-6^{-/-}* and *Tsg-6^{+/-}* mice 1 day after injury (Fig. 1A). The levels of *Ccl5* (*Rantes*) were also assessed 1, 5 and 10 days post-injury. There was a significant increase in the expression of *Rantes* in the injured hemisphere of *Tsg-6^{-/-}* mice when compared to *Tsg-6^{+/-}* mice (a four fold increase) 5 days after injury; however, no difference was found between *Tsg-6^{-/-}* and *Tsg-6^{+/-}* mice 1 and 10 days post-injury (Fig. 2D–F). *IL1β* levels were increased in the injury site of *TSG-6^{-/-}* mice when compared to *Tsg-6^{+/-}* mice at 1 day post-injury (Fig. 2G). At 5 days post-injury a threefold and fourfold increase in the expression of *IL1β* were noted in the injury site and remaining injured hemisphere, respectively, of *Tsg-6^{-/-}* mice when compared to *Tsg-6^{+/-}* mice (Fig. 2H). At 10 days post-injury, a 2.5-fold increase in the expression of *IL1β* was noted in the injury site of *Tsg-6^{-/-}* mice when compared to *Tsg-6^{+/-}* mice (Fig. 2I).

The effect of TSG-6 on the activation of microglia and infiltration of macrophages into the injury site after PBI

In order to assess the inflammatory response in *Tsg-6^{-/-}* and *Tsg-6^{+/-}* mice, we also evaluated the number of CD68⁺ cells present within the injury site at 3 days post-injury (Fig. 3A, C). CD68 is routinely used as a marker

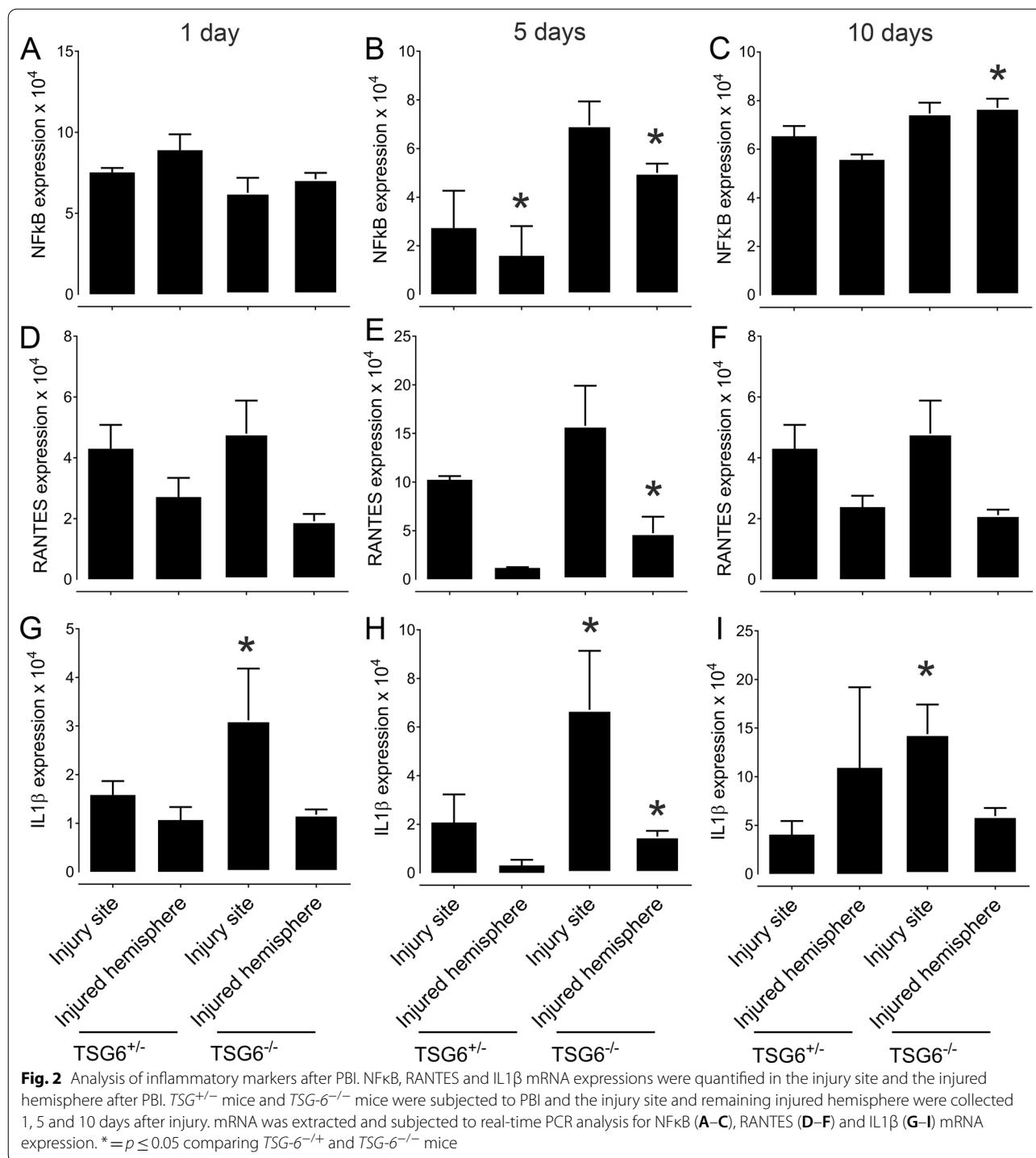
for macrophages and activated microglia. There was a significant increase in the number of CD68⁺ cells in and around the injury site of *Tsg-6^{-/-}* mice when compared to *Tsg-6^{+/-}* mice (Fig. 3A panels i and ii). Importantly, even when analyzing deeper regions of the injury site of *Tsg-6^{+/-}* mice, the level of CD68⁺ cell infiltration was not as intense as that observed in *Tsg-6^{-/-}* mice (Fig. 3A panel iii). The combined number of CD68⁺ cells in the injury site and within a range of 100 μm from the wound edge was counted from images obtained from 2 different sections from at least 5 mice from each experimental point (Fig. 3C). A two fold increase in CD68⁺ cells was found in *Tsg-6^{-/-}* mice when compared to *Tsg-6^{+/-}* mice (Fig. 3C).

Correlation between increased inflammatory response and neuronal damage

In order to verify whether the increased inflammatory response observed in *Tsg-6^{-/-}* mice correlates with neuronal loss, the distribution of neurons in and around the injury site was analyzed in *Tsg-6^{-/-}* and *Tsg-6^{+/-}* mice 14 days post-injury (Fig. 3B). For such, β III tubulin was used as a tissue-specific marker for identifying neurons within injured and non-injured brains. The distribution of β III tubulin can be seen in the equivalent region of uninjured *Tsg-6^{-/-}* and *Tsg-6^{+/-}* mice (Fig. 3 B panels i and ii). A significant increase in the area devoid of β III tubulin staining can be observed in and around the injury site of *Tsg-6^{-/-}* mice when compared to *Tsg-6^{+/-}* mice 14 days post-injury (Fig. 3B iii and iv). The relative fluorescence units (RLU) were quantified from an image of the injury site captured from at least 3 mice per experimental point. There was a fourfold decrease in β III tubulin staining in and around the injury site of *Tsg-6^{-/-}* mice when compared to *Tsg-6^{+/-}* mice 14 days post-injury (Fig. 3D).

The effect of TSG-6 on the secretion of glial scar components after PBI

We also evaluated glial scar secretion within the injury site and injured hemisphere by evaluating the expression levels of the biosynthetic enzymes responsible for HA and CS chain elongation, specifically hyaluronan synthase 2 (*Has2*), carbohydrate (chondroitin 4) sulfotransferase (*chst 11*) and carbohydrate (chondroitin 4) sulfotransferase 12 (*chst 12*) (Fig. 4). *Has2* expression increased in the injury site when compared to the remaining injured hemisphere 5 days post injury in both *Tsg-6^{+/-}* and *Tsg-6^{-/-}* mice, confirming the numerous previously published reports showing that HA is an integral component of the glial scar [17, 66–68]. Interestingly, there was a twofold increase in *Has2* expression in the injury site of *Tsg-6^{-/-}* mice when compared to *Tsg-6^{+/-}* mice 5 days



after injury, indicating that there is a higher rate of glial scar production in *Tsg-6^{-/-}* mice when compared to *Tsg-6^{+/-}* mice (Fig. 4A). At 10 days post-injury, *Has2* expression was still increased by twofold in *Tsg-6^{-/-}* mice when compared to *Tsg-6^{+/-}* mice, but at this time point there was also an increase in *Has2* expression in the remaining

injured hemisphere of *Tsg-6^{-/-}* mice when compared to *Tsg-6^{+/-}* mice (Fig. 4B). Thus, at 10 days after injury, in *Tsg-6^{-/-}* mice, the expression of glial scar components was no longer limited to the injury site, but was also present within the remaining injured hemisphere. Interestingly, this was also true for the expression of *Chst11* and

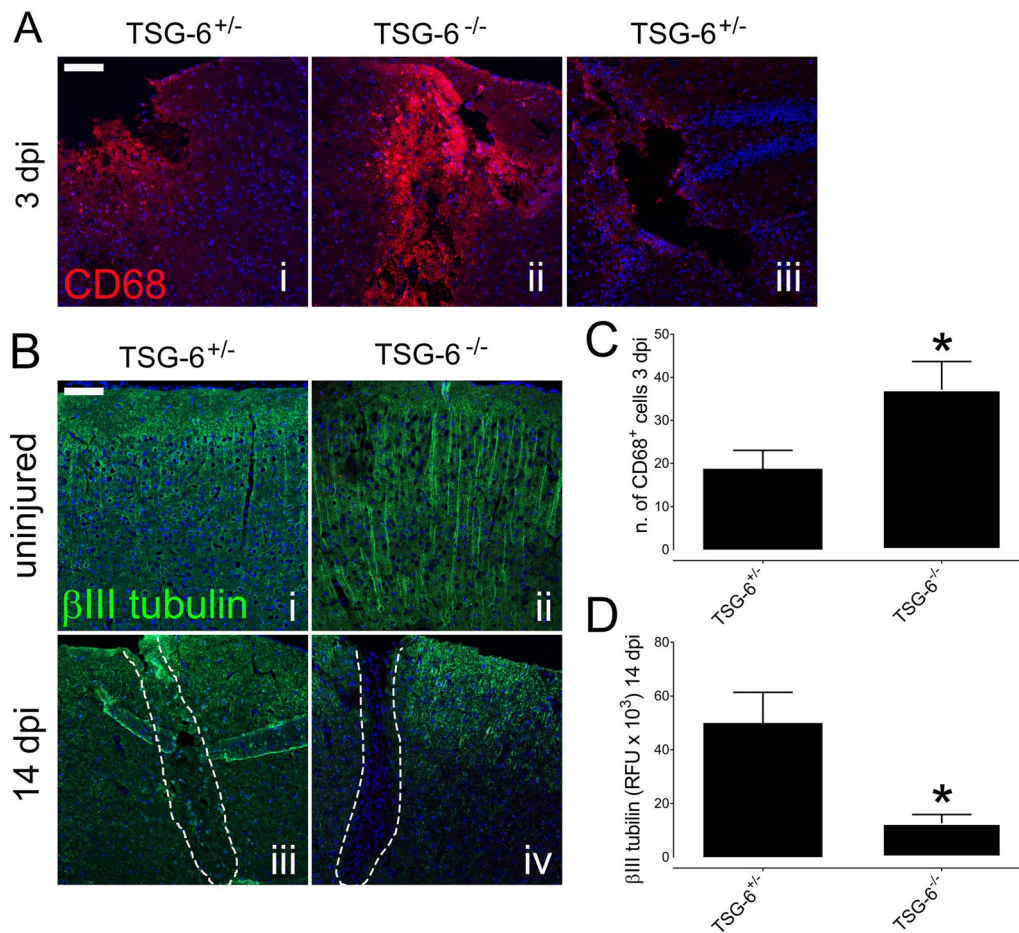


Fig. 3 Analysis of inflammatory cell infiltration and neuronal cell loss after PBI. The distribution of macrophages and activated microglia was evaluated within the injury site of TSG-6^{+/-} and TSG-6^{-/-} mice 3 days post-injury (dpi) by anti-CD68 immunostaining (red) (A). Neuronal cells were immunostained with anti-β III tubulin (green) in the equivalent area of uninjured TSG-6^{+/-} (i) and TSG-6^{-/-} (ii) mice and within the injury site of TSG-6^{+/-} (iii) and TSG-6^{-/-} (iv) mice 14 days post-injury (dpi). The number of CD68⁺ cells was counted in the injury site and within 100 μm of the wound edge of TSG-6^{+/-} and TSG-6^{-/-} mice 3 days post-injury (C). The relative fluorescent units (RFU) of anti-β III tubulin staining were quantified in and around the injury site of TSG-6^{+/-} and TSG-6^{-/-} mice 14 days post-injury (D). Nuclei were counterstained with DAPI. Scale bar represents 100 μm. * = $p \leq 0.05$ comparing TSG-6^{+/-} and TSG-6^{-/-} mice

Chst12, which showed a five fold and four fold increase, respectively, within the injured hemisphere of *Tsg-6*^{-/-} mice at 5 days post injury when compared to *Tsg-6*^{+/-} mice (Fig. 4C, E). The increase in *Chst11* and *Chst12*, in both the injury site and injured hemisphere, was maintained through to 10 days post-injury (Fig. 4D, F).

The effect of TSG-6 on astrocyte activation and recruitment after PBI

In order to further investigate the process of astrogliosis in *Tsg-6*^{+/-} and *Tsg-6*^{-/-} mice, injured brains were harvested and processed for histology. Sections were stained for GFAP in order to assess the distribution of astrocytes in and around the injury site, and, also, throughout the remaining brain tissue. The number

of astrocytes (GFAP⁺ cells) was counted within the injury site, throughout the injured hemisphere, and, also, throughout the contralateral hemisphere 3 and 14 days post-injury (Fig. 5A, B). At 3 and 14 days post-injury there was a significant increase in the number of astrocytes within the injury site when compared to the injured hemisphere and contralateral hemisphere in both *Tsg-6*^{+/-} and *Tsg-6*^{-/-} mice. At 3 days post-injury there was no significant difference between the number of astrocytes within the injury site between *Tsg-6*^{+/-} and *Tsg-6*^{-/-} mice; however, there was a significant increase in the number of astrocytes within the injured hemisphere in *Tsg-6*^{-/-} mice when compared to *Tsg-6*^{+/-} mice (Fig. 5A). At 14 days post-injury there was a significant increase in the number of astrocytes

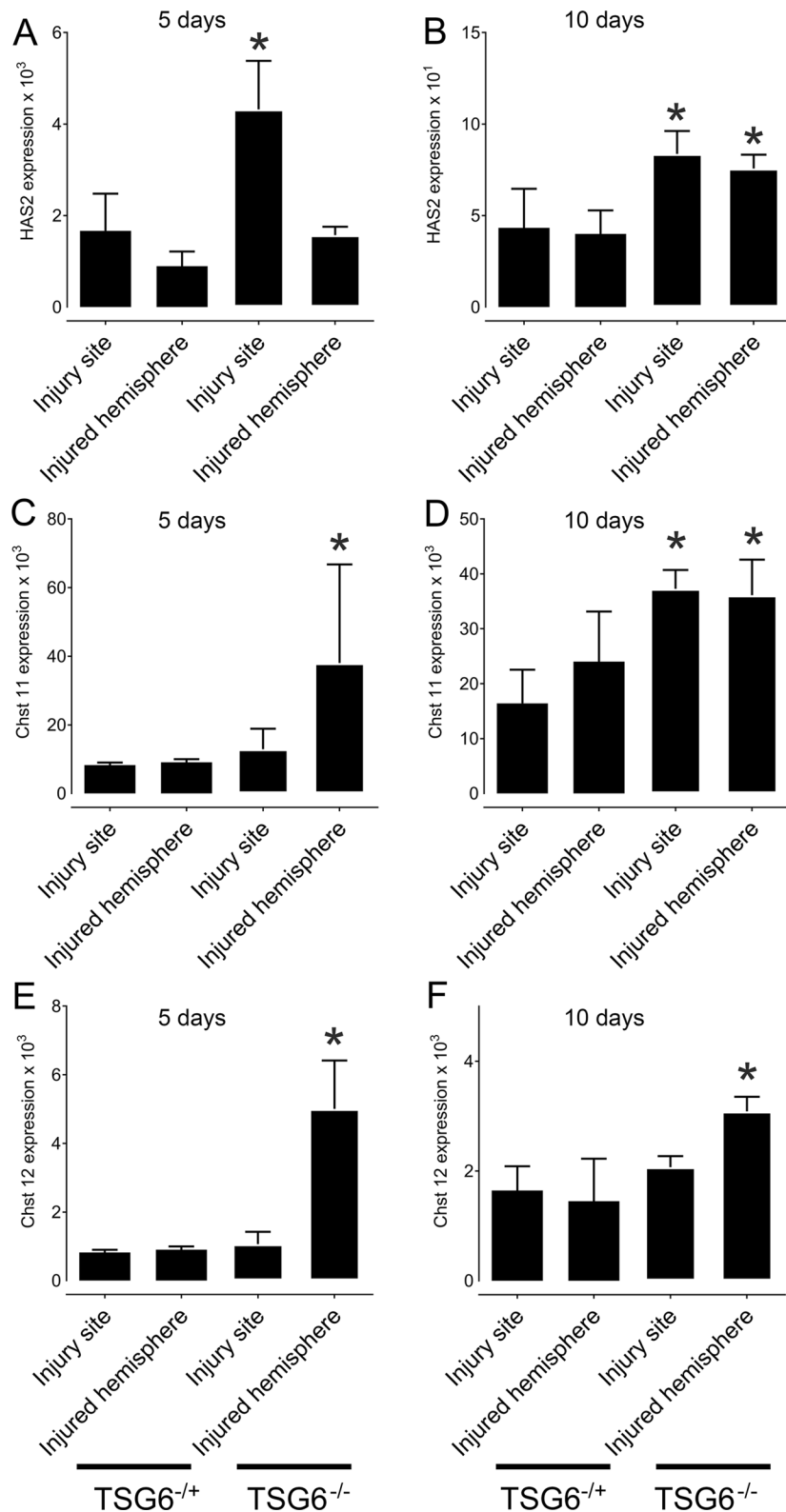


Fig. 4 Analysis of glial scar extracellular matrix components after PBI. HAS2, Chst 11 and Chst 12 mRNA expression levels were quantified in the injury site and the injured hemisphere after PBI. *TSG6^{+/+}* and *TSG6^{-/-}* mice were subjected to PBI, and the injury site and remaining injured hemisphere were collected 5 and 10 days after injury. mRNA was extracted and subjected to real-time PCR analysis for HAS2 (A, B), Chst11 (C, D) and Chst 12 (E, F) mRNA expression. * = $p \leq 0.05$ comparing *TSG6^{+/+}* and *TSG6^{-/-}* mice

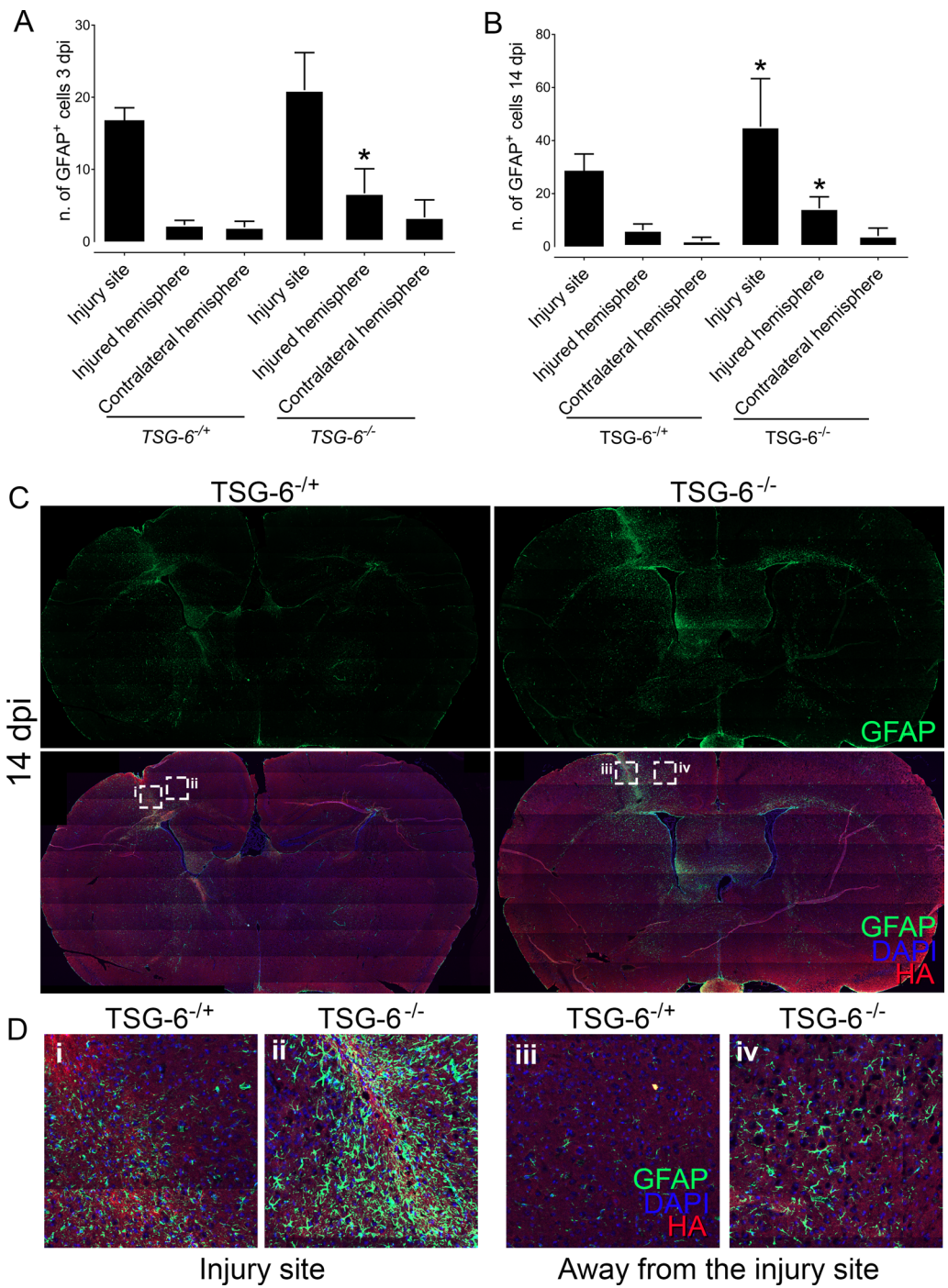


Fig. 5 Analysis of astrocyte activation and recruitment after PBI. Brain sections from *TSG-6^{+/-}* and *TSG-6^{-/-}* mice were analyzed by immunofluorescence. Astrocytes were identified with anti-GFAP (green) and the glial scar with HABP (red). Nuclei were counterstained with DAPI (blue). Z-stacks were captured of the entire brain section using the tiling mode, and images were stitched together using Zen software. Thereafter, the number of astrocytes was counted within the injury site, within the injured hemisphere and in the contralateral hemisphere of brains 3 (**A**) and 14 dpi (**B**) in a double blinded manner. The distribution of astrocytes throughout the brain sections shows that in *TSG-6^{-/-}* mice the increase in astrocytes is not restricted to the injury site (**C**). Magnified images of the areas demarcated in (**C**) can be seen in (**D**). At least 3 mice were analyzed per genotype for each time point. * = $p \leq 0.05$ comparing *TSG-6^{+/-}* and *TSG-6^{-/-}* mice

within the injury site and injured hemisphere in *Tsg-6^{-/-}* mice when compared to *Tsg-6^{+/-}* mice (Fig. 5B, D). The increase in astrocytes can be seen beyond the injury site in *Tsg-6^{-/-}* mice (Fig. 5C, D panel iv).

Discussion

Chondroitin sulfate proteoglycans (CSPGs) are well established as major extracellular matrix components in the central nervous system [69]. Over a decade ago, Silver et al. identified that CSPGs within the glial scar inhibit axonal growth, and this triggered a great deal of interest in targeting CS within the scar tissue as a means to promote axonal regeneration [32, 70–72]. Over the years, strategies utilizing the enzymes chondroitinase ABC (ChABC) and ChAC have been used to remove the CS component of the glial scar as a means to promote axonal growth and regeneration [50, 73–77]. Many studies have shown that specifically removing CS within the glial scar is enough for axons to grow across the injury site [32, 70, 78, 79]. However, significant regeneration was never observed in these studies, and many groups found limited or no improvement after targeting CS within the glial scar [70]. One unique characteristic of TSG-6 is its known ability to bind to a number of ligands including HA, CS and core proteins of proteoglycans (i.e. versican and aggrecan), forming specific HA/HC/TSG-6 and/or CS/HA/HC/TSG-6 matrices with immunosuppressive characteristics [61, 80–84]. Our previous study suggests these HA/HC/TSG-6 matrices are also present within the glial scar [48]. Therefore, given that TSG-6 directly binds to both HA and CS to form specific anti-inflammatory matrices, the ChABC and ChAC treatments used over the years to target the glial scar as a means to promote regeneration would also have removed TSG-6, a known anti-inflammatory molecule that is also a component of the glial scar [82]. The loss of TSG-6 by these treatments could, in part, explain why significant functional recovery was never obtained after ChABC and/or ChAC treatments.

To explore the role of TSG-6 in TBI, specifically in astrogliosis, we compared the differences in injury outcomes in *Tsg-6^{-/-}* and *Tsg-6^{+/-}* mice after PBIs. Our data show an increase in TSG-6 expression in the injured hemisphere of *Tsg-6^{+/-}* mice after TBI. This increase in expression of TSG-6 after CNS insults supports our earlier findings in a rat model that astrocytes secrete high levels of TSG-6 upon injury, which aids in the formation of a specialized HA/HC/TSG-6 matrix as part of an inflammatory response [48]. Since TSG-6 is known for having anti-inflammatory properties, to further study whether high levels of TSG-6 serve a purpose of rapidly suppressing inflammation after injury, we performed similar penetrating injuries in *Tsg-6^{-/-}* mice. We

used immunofluorescence and RNA expression analyses of inflammatory and glial scar markers to elucidate the outcome during the acute phase and chronic phase of TBI. During the acute phase after injury, the observed increase in astrocyte activation, inflammatory cell infiltration and expression of inflammatory cytokines in *Tsg-6^{-/-}* mice indicate that the loss of TSG-6 results in a greater inflammatory response. Moreover, during the chronic phase of injury, unrestricted inflammatory response was observed throughout the injured hemisphere and was not limited to the injury site, as is seen after normal glial scar formation. Thus, injured *Tsg-6^{-/-}* mice appear to experience more severe tissue damage than their *Tsg-6^{+/-}* counterpart, both within and around the injury site. Thus, the loss of TSG-6 allows the damage to spread from the injury site to neighboring healthy tissues. We postulate that the cause of such widespread damage is due to the lack of the specialized HA-TSG6 or HA/HC/TSG-6 matrix, which could possibly serve to stabilize the glial scar and form an immunosuppressive environment, thereby protecting adjacent tissue from further damage. This hypothesis is further supported by the increase in CSPG and HA biosynthesis, both glial scar components, in *Tsg-6^{-/-}* mice. Specifically, these mice show increased *Has2*, *Chst11* and *Chst12* expression levels in tissues collected after the onset of glial scarring, and, also, during the chronic phase of astrogliosis, indicating an increase in scar tissue formation. This increase in expression was not only observed at the injury site, but also throughout the whole injured hemisphere, suggesting that the tissue damage spreads beyond the injury site in the absence of TSG-6. Collectively, these results demonstrate that the loss of TSG-6 leads to a more severe inflammatory response and, consequently, increased scarring after TBI. Thus, our results support the hypothesis put forward by many groups over the past decade that preventing the formation of the glial scar leads to inflammation and damage beyond the injury site. We also provide experimental evidence that shows that the glial scar functions to restrict the damage to the injury site. Importantly, these findings should be taken into account when attempts are made to disrupt the glial scar as a means to promote neuronal regeneration, since preventing formation of the glial scar may not have the beneficial outcomes as previously presumed.

Conclusion

Our results show that TSG-6 has an anti-inflammatory role in the glial scar. Our study further supports the hypothesis that the glial scar forms a protective border surrounding the injury site thereby preventing the

spread of inflammation and damage beyond the injury site.

Methods

TSG6 null (TSG6^{-/-}) or heterozygous (TSG6^{+/-}) mice and animal maintenance

Transgenic *Tsg-6 null* mice (*Tnfr16^{Δ/Δ}*), herein referred to as *Tsg-6^{-/-}* mice, and heterozygous mice, herein referred to as *Tsg-6^{+/-}* mice, were maintained as previously described [56]. Our previously published work demonstrated that *Tsg-6^{+/-}* mice present a similar distribution of astrocytes throughout the brain to wild-type (wt) mice [48]. Moreover, *Tsg-6^{+/-}* mice have previously been shown not to display a phenotype and present similar TSG-6 expression levels as wt mice, and were therefore used as littermate controls in our study [56]. Experimental procedures for handling the mice were approved by the Institutional Animal Care and Use Committee (IACUC), University of Houston under protocol 16-036.

Brain injury

Mice (7 to 8 weeks old) were anesthetized with ketamine (80–100 mg/kg—Vedco INC, Catalog# 07-890-8598) and xylazine (5–10 mg/kg, Akorn INC, Catalog# 07-808-1947) by IP injection and allowed to go into full anesthetic state. A sterile surgical drill (Precision Tools, Model Craft PPV2237) was used to make a hole of approximately 1.5 mm in diameter in the skull over the right frontal cortex at the stereotaxic coordinates AP: 1.0 mm, ML: 1.5 mm, and DV: 1.5 mm, according to Franklin and Paxinos (85). A 30-gauge needle (Exel, Catalog# 26437) was then used to make a puncture wound at a depth of 2 mm. After injury, the skin at the surgical site was closed with two sutures. The area was then cleaned with 70% ethanol, and mice were placed on a heating pad and monitored until they regained consciousness prior to being transferred to a clean cage. All surgeries were carried out at the same time of day to minimize bias. Mice were monitored daily and did not show any decrease in weight $\geq 15\%$ when compared to their pre-surgical weight. Mice were euthanized, as outlined below, at 1, 3 and 5 days post injury to study the acute effects of brain injury, and at 10 and 14 days to study long-term/chronic effects. Five mice per experimental group were used for the real-time PCR analysis and at least seven mice per experimental group were used for immunofluorescence analysis.

Perfusion fixation and brain tissue processing

Brain samples were collected at 1, 3, 5, 10, and 14 days post injury for immunofluorescence analyses. Briefly, mice were initially injected with a lethal dose of

combined anesthetics containing 200 mg of ketamine and 40 mg xylazine. Final dosage received was 3 mg of ketamine and 0.6 mg of xylazine per mouse. Once mice were under deep anesthesia, abdominal and thoracic excisions were performed to expose the heart, which was used to perfuse 2% formalin (Fisher Scientific, Catalog# SF100-4) throughout the whole body via a gravity-driven flow system for whole body fixation. Subsequently, the brain was isolated from the skull and further immerse fixed for 2 days in 2% paraformaldehyde (Electron Microscopy Sciences, Catalog# 15710). For cryosection processing, brains were immersed in 30% sucrose for 2 days, embedded in OCT embedding medium (Fisher Healthcare, Catalog# 4585) and frozen. Sections 10 μm thick were obtained, mounted on superfrost slides (VWR, Catalog# 48311-703) and stored at $-20\text{ }^{\circ}\text{C}$ until use.

Immunofluorescence

Upon use, the slides were heated at $65\text{ }^{\circ}\text{C}$ for 30 min and, subsequently, sections were washed with PBS to remove tissue freezing medium. Sections were then treated with 0.1% glycine (Fisher Chemical, Catalog# G46-500), blocked with 5% FBS (Seradigm, Catalog# 3100-500) and permeabilized with 0.1% saponin prepared in PBS. Sections were then incubated with the primary antibodies anti-Tenascin (Abcam, Ab108930), anti-GFAP (Abcam, Ab4647), anti-CD68 (Abcam, Ab31630) and anti- β III tubulin (Covance, PRB-435P-100). Sections were washed and incubated with appropriate secondary donkey antibodies conjugated with Alexa Fluor[®] 488 (Life Technologies) or Alexa Fluor[®] 555 (Life Technologies) for one hour at $18\text{ }^{\circ}\text{C}$. For HA staining, tissues were incubated with biotinylated HA binding protein (385911, Millipore) followed by NeutrAvidin[®] Alexa 555 (Life Technologies). The tissues were then washed and nuclei stained with 4',6-diamidino-2-phenylindole (DAPI, Sigma-Aldrich). Sections were mounted in Prolong[®]Gold (Molecular Probes) and imaged using a ZEISS LSM 800 Confocal microscope with Airyscan. Secondary controls were done with a goat IgG isotype control (ab37388; Abcam) in place of the primary antibody and did not yield any significant staining (results not shown). For imaging, multiple z-stack tiles were captured of entire brain sections and frames were processed together into a single image (using the stitching mode followed by full orthogonal projection) using Zen Software (Zeiss). The number of GFAP⁺ and CD68⁺ cells in and around the injury site were counted by two independent investigators in a blinded manner and the relative Fluorescent intensity was measured using the Zen Software (Zeiss).

Table 1 Primers used for real time PCR analysis

Gene (<i>Mus musculus</i>)	Accession number	Forward (5' → 3')	Reverse (5' → 3')
Tenascin C (tnc)	NM_011607.3	CCAGGGTTGCCACCTATTT	GTCTAGAGGATCCCCTACTACTT
Gfap	NM_001131020.1	AACAACCTGGCTGCGTATAG	TCTCGAACTCCTCCTCATAGAT
Tsg-6 /Tnfaip6	NM_009398.2	CCCACATGCAAAGGAGTGTG	TGAGCCGAATGTGCCAGTAG
Chst1	NM_021439.2	CACCCAGTCATGCGGAGGAA	GCAGGATGGCAGTGTGGAT
Chst12	NM_021528.3	GAGCTGGAGAACGAAGATTTT	CAGGAGTACTGGATGAAGTTG
IL1β	NM_008361.4	GTGCAAGTGTCTGAAGCAGC	CTCATCACTGTCAAAGGTGGC
Cspg4	NM_139001.2	TCTACAGCTCCTGCCTCCTT	ATGTGGAGAAGTGGAGCAGC
Ccl5 (Rantes)	NM_013653.3	CCTCACCATATGGCTCGGAC	ACGACTGCAAGATGGAGCA
Nfkb1	NM_008689.2	GTCACCCATGGCACCATAAA	CCTTCACCTTCAGTTTCTTCTC
Has1	NM_008215.2	CTA TGC TAC CAA GTA TAC CTC G	TCT CGG AAG TAA GAT TTG GAC
Has2	NM_008216.3	CGG TCG TCT CAA ATT CAT CTG	ACA ATG CAT CTT GTT CAG CTC
Has 3	NM_008217.4	GAT GTC CAA ATC CTC AAC AAG	CCC ACT AAT ACA TTG CAC AC
Itih1		CCA CCC CAT CGG TTT TGA AGT GTC T	TGC CAC GGG TCC TTG CTG TAG TCT
Itih2		ATG AAA AGA CTC ACG TGC TTT TTC	ATT TGC CTG GGG CCA GT
Itih3		TGA GGA GGT GGC CAA CCC ACT	CGC TTC TCC AGC AGC TGC TC
Actb	NM_007393.5	CACTGTCGAGTCGCGTCC	TCATCCATGGCGAACTGGTG
Gapdh	NM_001289726.1	AACAGCAACTCCCACTCTTC	CCTGTTGCTGTAGCCGTATT

At least 2 sections were scanned and analyzed from each animal for each set of antibodies and representative images shown in the figures.

RNA extraction from brains and real-time PCR analysis

Brains collected from injured mice at 1, 5 and 10 days post injury were used for RNA extraction. At least 5 mice were used per experimental group and each animal was analyzed separately. Briefly, mice were euthanized and brain tissue was immediately isolated from each mouse. Injury sites (A samples) were dissected from the rest of the injured right hemisphere, transferred into a labeled Eppendorf tube and immediately immersed in liquid nitrogen. The remaining right hemisphere brain tissue (B samples) from each animal was transferred into a different tube and frozen as described. The samples were kept at -80°C until RNA extraction. Total RNA was isolated from these tissue samples using Trizol[®] Reagent (Invitrogen, Carlsbad, CA) and chloroform extraction (Sigma-Aldrich, Catalog# 650498). First strand cDNA was reverse transcribed using 1.5 to 2 μg of total RNA and the high capacity cDNA Reverse Transcription kit (Applied Biosystems, catalog# 4368814, lot 00593854), according to the manufacturer's instructions. Quantitative real-time PCR amplification was performed on 1 μg or 50 ng of the cDNA (1:5) using the PowerUp SYBR Green Master Mix kit (Applied Biosystems, Catalog# A25918) in a CFX Connect Real-time System from BIO-RAD, using an activation cycle of 95°C for 10 min, 40 cycles

of 95°C for 15 s and 60°C for 1 min. A complete list of primers used in this study is shown in Table 1. Gene expression levels were normalized against *Actb* and *Gapdh* using the $2^{-\Delta\text{Ct}}$ and/or $2^{-\Delta\Delta\text{Ct}}$ methods.

Statistical analysis

All values are presented as the mean \pm standard deviation of the mean. The difference between the two groups was compared by means of the Student's t-test. $p \leq 0.05$ was considered to be statistically significant. Statistical analysis was performed using the GraphPad Prism version 7 software package (GraphPad Software, San Diego, CA, USA). * was used to indicate statistical differences of ≤ 0.05 . Unless indicated otherwise, * indicates the statistical difference of *Tsg-6*^{-/-} mice compared to *Tsg-6*^{+/-} mice for each time point.

Abbreviations

TBI: Traumatic brain injury; TNF: Tumor necrosis factor; TSG-6: TNF-stimulated gene-6; GFAP: Glial fibrillary acidic protein; VIM: Vimentin; CSPGs: Chondroitin sulfate proteoglycans; STAT3: Signal transducer and activator of Transcription 3; HA: Hyaluronan; GAGs: Glycosaminoglycans; CNS: Central nervous system; HC: Heavy chain; ITI or Ial: Inter-alpha inhibitor; hUMSCs: Human umbilical cord mesenchymal stem cells; PTX3: Pentraxin-3; NFKB: Nuclear factor kappa-light-chain-enhancer; IL1β: Interleukin 1 beta; Ccl5: Chemokine (C-C motif) ligand 1 or Rantes; HAS: Hyaluronan synthase; Chst: Carbohydrate (chondroitin 4) sulfotransferase.

Acknowledgements

The authors would like to thank Denise Lerma, Nicole Grimmes and Garrett Elliot who contributed in the early stages of the study. The authors are in debt to Tarsis F. Gesteira and Yvette May Coulson-Thomas for their invaluable discussions and suggestions throughout the study. Transgenic *Tsg-6 null* mice (*Tnfrp6*^{ΔΔ}) were kindly provided by Dr. Mark Lauer.

Authors' contributions

VH and VJCT generated the hypothesis and experimental design. VJCT, KNM and MS contributed to the experimental design. KNM, MS, AN and VJCT conducted the experiments and helped with the data analysis. KNM and VJCT wrote the manuscript. KNM, MS, AN, SP, VH and VCT read and approved the final manuscript.

Funding

This study was supported by start-up funds from the University of Houston to VJCT, The Mizutani Foundation grant to VJCT and the National Institute of Health/National Eye Institute R01 EY029289 to VJCT and Core grant P30 EY07551.

Availability of data and materials

The datasets used and/or analyzed during the current study are available from the corresponding author on reasonable request.

Declarations

Ethics approval and consent to participate

Experimental procedures for handling the mice and animal care were in accordance to regulations of the National Institute of Health and were approved by the Institutional Animal Care and Use Committee, University of Houston under protocols 16-025, 16-035, 16-036, 16-044.

Consent to publish

The authors grant their consent to publish the material presented herein.

Competing interests

The authors declare that they have no competing interests.

Author details

¹College of Optometry, University of Houston, 4901 Calhoun Road, Houston, TX 77204-2020, USA. ²Cleveland Clinic, Cleveland, OH, USA. ³Present Address: Department of Bioengineering, Rice University, Houston, TX 77030, USA.

Received: 21 April 2020 Accepted: 9 July 2021

Published online: 04 August 2021

References

- Hyder AA, Wunderlich CA, Puvanachandra P, Gururaj G, Kobusingye OC. The impact of traumatic brain injuries: a global perspective. *NeuroRehabilitation*. 2007;22:341–53.
- Bose P, Hou J, Thompson FJ. Traumatic brain injury (TBI)-induced spasticity: neurobiology, treatment, and rehabilitation. *Brain Neurotrauma: Molecular, Neuropsychological, and Rehabilitation Aspects*. 2015.
- Blennow K, Brody DL, Kochanek PM, Levin H, McKee A, Ribbers GM, et al. Traumatic brain injuries. *Nat Rev Dis Prim*. 2016;2:1–19.
- Graham DI, McIntosh TK, Maxwell WL, Nicoll JAR. Recent advances in neurotrauma. *J Neuropathol Exp Neurol*. 2000;59:641–51.
- Zaninotto ALC, Costa BT, Ferreira IS, French M, Paiva WS, Fregni F. Traumatic brain injury. In: *NeuroMethods*. 2018.
- Burda JE, Bernstein AM, Sofroniew MV. Astrocyte roles in traumatic brain injury. *Exp Neurol*. 2016;275:305–15.
- Gugliandolo E, D'Amico R, Cordaro M, Fusco R, Siracusa R, Crupi R, et al. Neuroprotective effect of artesunate in experimental model of traumatic brain injury. *Front Neurol*. 2018;9:590.
- Kovacs SK, Leonessa F, Ling GSF. Blast TBI models, neuropathology, and implications for seizure risk. *Front Neurol*. 2014;5:47.
- Sharp DJ, Scott G, Leech R. Network dysfunction after traumatic brain injury. *Nat Rev Neurosci*. 2014;10:156–66.
- Fakhran S, Alhilali L. Neurodegenerative changes after mild traumatic brain injury. In: *Concussion*. 2012.
- Nagahiro S, Mizobuchi Y. Current topics in sports-related head injuries: a review. *Neurol Med Chir (Tokyo)*. 2014.
- Jordan BD. The clinical spectrum of sport-related traumatic brain injury. *Nat Rev Neurosci*. 2013;9:222–30.
- Costanza A, Weber K, Gandy S, Bouras C, Hof PR, Giannakopoulos P, et al. Review: contact sport-related chronic traumatic encephalopathy in the elderly: clinical expression and structural substrates. *Neuropathol Appl Neurobiol*. 2011;27:570–84.
- McAllister T, McCrea M. Long-term cognitive and neuropsychiatric consequences of repetitive concussion and head-impact exposure. *J Athl Train*. 2017;52:309–17.
- Sofroniew MV, Vinters HV. Astrocytes: biology and pathology. *Acta Neuropathol*. 2010;119:7–35.
- Sofroniew MV. Astroglialosis. *Cold Spring Harb Perspect Biol*. 2015;7:a020420.
- George N, Geller HM. Extracellular matrix and traumatic brain injury. *J Neurosci Res*. 2018;96:573–88.
- Siracusa R, Fusco R, Cuzzocrea S. Astrocytes: role and functions in brain pathologies. *Front Pharmacol*. 2019;10:1114.
- Zhou Y, Shao A, Yao Y, Tu S, Deng Y, Zhang J. Dual roles of astrocytes in plasticity and reconstruction after traumatic brain injury. *Cell Commun Signal*. 2020;18:1–16.
- Sofroniew MV. Reactive astrocytes in neural repair and protection. *Neuroscientist*. 2005;11:400–7.
- Smith PD, Coulson-Thomas VJ, Foscarin S, Kwok JCF, Fawcett JW. "GAG-ing with the neuron": the role of glycosaminoglycan patterning in the central nervous system. *Exp Neurol*. 2015;274:100–14.
- McGraw J, Hiebert GW, Steeves JD. Modulating astroglialosis after neuro-trauma. *J Neurosci Res*. 2001;63:109–15.
- Kawano H, Kimura-Kuroda J, Komuta Y, Yoshioka N, Li HP, Kawamura K, et al. Role of the lesion scar in the response to damage and repair of the central nervous system. *Cell Tissue Res*. 2012;349:169–80.
- Burda JE, Sofroniew MV. Reactive gliosis and the multicellular response to CNS damage and disease. *Neuron*. 2014;81:229–48.
- Sofroniew MV. Molecular dissection of reactive astroglialosis and glial scar formation. *Trends Neurosci*. 2009;32:638–47.
- Okada S, Hara M, Kobayakawa K, Matsumoto Y, Nakashima Y. Astrocyte reactivity and astroglialosis after spinal cord injury. *Neurosci Res*. 2018;126:39–43.
- Davies SJA, Goucher DR, Doller C, Silver J. Robust regeneration of adult sensory axons in degenerating white matter of the adult rat spinal cord. *J Neurosci*. 2018;38:5810–22.
- McKeon RJ, Jurynek MJ, Buck CR. The chondroitin sulfate proteoglycans neurocan and phosphacan are expressed by reactive astrocytes in the chronic CNS glial scar. *J Neurosci*. 2018;38:10778–88.
- Okada S, Nakamura M, Katoh H, Miyao T, Shimazaki T, Ishii K, et al. Conditional ablation of Stat3 or Socs3 discloses a dual role for reactive astrocytes after spinal cord injury. *Nat Med*. 2006;12:829–34.
- Fitch MT, Doller C, Combs CK, Landreth GE, Silver J. Cellular and molecular mechanisms of glial scarring and progressive cavitation: In vivo and in vitro analysis of inflammation-induced secondary injury after CNS trauma. *J Neurosci*. 1999;19:8182–98.
- Vogelaar CF, König B, Krafft S, Estrada V, Brazda N, Ziegler B, et al. Pharmacological suppression of CNS scarring by deferroxamine reduces lesion volume and increases regeneration in an in vitro model for astroglial-fibrotic scarring and in rat spinal cord injury in vivo. *PLoS ONE*. 2015;10:e0134371.
- Silver J, Miller JH. Regeneration beyond the glial scar. *Nat Rev Neurosci*. 2004;5:146–56.
- Galtrey CM, Fawcett JW. The role of chondroitin sulfate proteoglycans in regeneration and plasticity in the central nervous system. *Brain Res Rev*. 2007;54:1–18.
- Lin CM, Lin JW, Chen YC, Shen HH, Wei L, Yeh YS, Chiu WT. Hyaluronic acid inhibits the glial scar formation after brain damage with tissue loss in rats. *Surg Neurol*. 2009;72:S50–4.
- Gesteira TF, Coulson-Thomas YM, Coulson-Thomas VJ. Anti-inflammatory properties of the glial scar. *Neural Regen Res*. 2016;11:1742.
- Voskuhl RR, Peterson RS, Song B, Ao Y, Morales LBJ, Tiwari-Woodruff S, et al. Reactive astrocytes form scar-like perivascular barriers to leukocytes during adaptive immune inflammation of the CNS. *J Neurosci*. 2009;29:11511–22.
- Wanner IB, Anderson MA, Song B, Levine J, Fernandez A, Gray-Thompson Z, et al. Glial scar borders are formed by newly proliferated, elongated astrocytes that interact to corral inflammatory and fibrotic cells via

- STAT3-dependent mechanisms after spinal cord injury. *J Neurosci*. 2013;33:12870–86.
38. Faulkner JR. Reactive astrocytes protect tissue and preserve function after spinal cord injury. *J Neurosci*. 2004;24:2143–55.
 39. Myer DJ, Gurkoff GG, Lee SM, Hovda DA, Sofroniew MV. Essential protective roles of reactive astrocytes in traumatic brain injury. *Brain*. 2006;129:2761–72.
 40. Fitch MT, Silver J. CNS injury, glial scars, and inflammation: inhibitory extracellular matrices and regeneration failure. *Exp Neurol*. 2008;209:294–301.
 41. Bush TG, Puvanachandra N, Horner CH, Polito A, Ostensfeld T, Svendsen CN, et al. Leukocyte infiltration, neuronal degeneration, and neurite outgrowth after ablation of scar-forming, reactive astrocytes in adult transgenic mice. *Neuron*. 1999;23:297–308.
 42. Wilhelmsson U. Absence of glial fibrillary acidic protein and vimentin prevents hypertrophy of astrocytic processes and improves post-traumatic regeneration. *J Neurosci*. 2004;24:5016–21.
 43. Pekny M, Johansson CB, Eliasson C, Stakeberg J, Wallén Å, Perlmann T, et al. Abnormal reaction to central nervous system injury in mice lacking glial fibrillary acidic protein and vimentin. *J Cell Biol*. 1999;145:503–14.
 44. Pekny M. Astrocytic intermediate filaments: lessons from GFAP and vimentin knock-out mice. *Prog Brain Res*. 2001;132:23–30.
 45. Faulkner JR, Herrmann JE, Woo MJ, Tansey KE, Doan NB, Sofroniew MV. Reactive astrocytes protect tissue and preserve function after spinal cord injury. *J Neurosci*. 2004;24:2143–55.
 46. Herrmann JE, Imura T, Song B, Qi J, Ao Y, Nguyen TK, et al. STAT3 is a critical regulator of astrogliosis and scar formation after spinal cord injury. *J Neurosci*. 2008;28:7231–43.
 47. Fan H, Zhang K, Shan L, Kuang F, Chen K, Zhu K, et al. Reactive astrocytes undergo M1 microglia/macrophage-induced necroptosis in spinal cord injury. *Mol Neurodegen*. 2016;11:1–16.
 48. Coulson-Thomas VJ, Lauer ME, Soleman S, Zhao C, Hascall VC, Day AJ, et al. TSG-6 is constitutively expressed in adult CNS and associated with astrocyte-mediated glial scar formation following spinal cord injury. *J Biol Chem*. 2016;291:19939–52.
 49. Milner CM, Day AJ. TSG-6: a multifunctional protein associated with inflammation. *J Cell Sci*. 2003;116(10):1863–73.
 50. Bradbury EJ, Moon LDF, Popat RJ, King VR, Bennett GS, Patel PN, et al. Chondroitinase ABC promotes functional recovery after spinal cord injury. *Nature*. 2002;416:636–40.
 51. Massey JM, Hubscher CH, Wagoner MR, Decker JA, Amps J, Silver J, et al. Chondroitinase ABC digestion of the perineuronal net promotes functional collateral sprouting in the cuneate nucleus after cervical spinal cord injury. *J Neurosci*. 2006;26:4406–14.
 52. Carrette O, Nemade RV, Day AJ, Brickner A, Larsen WJ. TSG-6 is concentrated in the extracellular matrix of mouse cumulus oocyte complexes through hyaluronan and inter-alpha-inhibitor binding. *Biol Reprod*. 2001;65:301–8.
 53. Salustri A, Yanagishita M, Hascall VC. Synthesis and accumulation of hyaluronic acid and proteoglycans in the mouse cumulus cell-oocyte complex during follicle-stimulating hormone-induced mucification. *J Biol Chem*. 1989;264:13840–7.
 54. Salustri A, Yanagishita M, Underhill CB, Laurent TC, Hascall VC. Localization and synthesis of hyaluronic acid in the cumulus cells and mural granulosa cells of the preovulatory follicle. *Dev Biol*. 1992;151:541–51.
 55. Camaioni A, Hascall VC, Yanagishita M, Salustri A. Effects of exogenous hyaluronic acid and serum on matrix organization and stability in the mouse cumulus cell-oocyte complex. *J Biol Chem*. 1993;268:20473–81.
 56. Fulop C. Impaired cumulus mucification and female sterility in tumor necrosis factor-induced protein-6 deficient mice. *Development*. 2003;130:2253–61.
 57. Stober VP, Johnson CG, Majors A, Lauer ME, Cali V, Midura RJ, et al. TNF-stimulated gene 6 promotes formation of hyaluronan-inter-alpha-inhibitor heavy chain complexes necessary for ozone-induced airway hyperresponsiveness. *J Biol Chem*. 2017;292:20845–58.
 58. Lauer ME, Glant TT, Mikecz K, DeAngelis PL, Haller FM, Husni ME, et al. Irreversible heavy chain transfer to hyaluronan oligosaccharides by tumor necrosis factor-stimulated gene-6. *J Biol Chem*. 2013;288:205–14.
 59. Petrey AC, De La Motte CA. Thrombin cleavage of inter-alpha-inhibitor heavy chain 1 regulates leukocyte binding to an inflammatory hyaluronan matrix. *J Biol Chem*. 2016;291:24324–34.
 60. Hill DR, Rho HK, Kessler SP, Amin R, Homer CR, McDonald C, et al. Human milk hyaluronan enhances innate defense of the intestinal epithelium. *J Biol Chem*. 2013;288:29090–104.
 61. Baranova NS, Foulcer SJ, Briggs DC, Tilakaratna V, Enghild JJ, Milner CM, et al. Inter-alpha-inhibitor impairs TSG-6-induced hyaluronan cross-linking. *J Biol Chem*. 2013;288:29642–53.
 62. Kessler SP, Obery DR, De La Motte C. Hyaluronan synthase 3 null mice exhibit decreased intestinal inflammation and tissue damage in the DSS-induced colitis model. *Int J Cell Biol*. 2015.
 63. Lim Y, Bendelja K, Opal SM, Siryaporn E, Hixson DC, Palardy JE. Correlation between mortality and the levels of inter-alpha inhibitors in the plasma of patients with severe sepsis. *J Infect Dis*. 2003;188:919–26.
 64. Schmidt EP, Overdier KH, Sun X, Lin L, Liu X, Yang Y, et al. Urinary glycosaminoglycans predict outcomes in septic shock and acute respiratory distress syndrome. *Am J Respir Crit Care Med*. 2016;194:439–49.
 65. Coulson-Thomas VJ, Gesteira TF, Hascall V, Kao W. Umbilical cord mesenchymal stem cells suppress host rejection: the role of the glyco-calyx. *J Biol Chem*. 2014;289:23465–81.
 66. Olté LS, Mendichi R, Kogan G, Schiller J, Stankovská M, Arnholt J. Degradative action of reactive oxygen species on hyaluronan. 2006; Available from: <https://pubs.acs.org/sharingguidelines>.
 67. Wight TN. Provisional matrix: a role for versican and hyaluronan [Internet]. Vols. 60–61, Matrix Biology. Elsevier B.V.; 2017 [cited 2021 Jan 15]. p. 38–56. Available from: [/pmc/articles/PMC5438907/?report=abstract](https://pubs.acs.org/sharingguidelines).
 68. Cicanic M, Sykova E, Vargova L, Braňl I. “Superglue” for the extracellular matrix in the brain white matter. *Int J Biochem Cell*. 2012;44:596–9.
 69. Dyck SM, Karimi-Abdolrezaee S. Chondroitin sulfate proteoglycans: Key modulators in the developing and pathologic central nervous system. *Exp Neurol*. 2015;269:169–87.
 70. McKeon RJ, Höke A, Silver J. Injury-induced proteoglycans inhibit the potential for laminin-mediated axon growth on astrocytic scars. *Exp Neurol*. 1995;136:32–43.
 71. Bradbury EJ, Carter LM. Manipulating the glial scar: chondroitinase ABC as a therapy for spinal cord injury. *Brain Res Bull*. 2011;84:306–16.
 72. McKeon RJ, Schreiber RC, Rudge JS, Silver J. Reduction of neurite outgrowth in a model of glial scarring following CNS injury is correlated with the expression of inhibitory molecules on reactive astrocytes. *J Neurosci*. 1991;11:3398–411.
 73. Foerster AP. Spontaneous regeneration of cut axons in adult rat brain. *J Comp Neurol*. 1982;210(4):335–56.
 74. Brückner G, Bringmann A, Härtig W, Köppe G, Delpech B, Brauer K. Acute and long-lasting changes in extracellular-matrix chondroitin-sulphate proteoglycans induced by injection of chondroitinase ABC in the adult rat brain. *Exp Brain Res*. 1998;121(3):300–10.
 75. Filous AR, Miller JH, Coulson-Thomas YM, Horn KP, Allain WJ, Silver J. Immature astrocytes promote CNS axonal regeneration when combined with chondroitinase ABC. *Dev Neurobiol*. 2010;70(12):826–41.
 76. Moon LDF, Asher RA, Rhodes KE, Fawcett JW. Regeneration of CNS axons back to their target following treatment of adult rat brain with chondroitinase ABC. *Nat Neurosci*. 2001;4:465–6.
 77. Elkin BS, Shaik MA, Morrison B. Chondroitinase ABC reduces brain tissue swelling in vitro. *J Neurotrauma*. 2011;28(11):2277–85.
 78. Busch SA, Silver J. The role of extracellular matrix in CNS regeneration. *Curr Opin Neurobiol*. 2007;17:120–7.
 79. Klappa N, Hermanns S, Straten G, Masannek C, Duis S, Hamers FPT, et al. Suppression of fibrous scarring in spinal cord injury of rat promotes long-distance regeneration of corticospinal tract axons, rescue of primary motoneurons in somatosensory cortex and significant functional recovery. *Eur J Neurosci*. 2005;22:3047–58.
 80. Milner CM, Tongsoongnoen W, Rugg MS, Day AJ. The molecular basis of inter-alpha-inhibitor heavy chain transfer on to hyaluronan: Figure 1. *Biochem Soc Trans*. 2007;35:672–6.
 81. Getting SJ, Mahoney DJ, Cao T, Rugg MS, Fries E, Milner CM, et al. The link module from human TSG-6 inhibits neutrophil migration in a hyaluronan- and inter-alpha-inhibitor-independent manner. *J Biol Chem*. 2002;277:51068–76.
 82. Baranova NS, Nilebäck E, Haller FM, Briggs DC, Svedhem S, Day AJ, et al. The inflammation-associated protein TSG-6 cross-links hyaluronan via hyaluronan-induced TSG-6 oligomers. *J Biol Chem*. 2011;286:25675–86.
 83. Higman VA, Briggs DC, Mahoney DJ, Blundell CD, Sattelle BM, Dyer DP, et al. A refined model for the TSG-6 link module in complex with

hyaluronan: use of defined oligosaccharides to probe structure and function. *J Biol Chem.* 2014;289:5619–34.

84. Martin J, Midgley A, Meran S, Woods E, Bowen T, Phillips AO, et al. Tumor necrosis factor-stimulated gene 6 (TSG-6)-mediated interactions with the inter- α -inhibitor heavy chain 5 facilitate tumor growth factor β 1 (TGF β 1)-dependent fibroblast to myofibroblast differentiation. *J Biol Chem.* 2016;291:13789–801.

85. Franklin KBJ, Paxinos G. The mouse brain in stereotaxic coordinates (map). Boston: Academic Press; 2007.

Publisher's Note

Springer Nature remains neutral with regard to jurisdictional claims in published maps and institutional affiliations.

Ready to submit your research? Choose BMC and benefit from:

- fast, convenient online submission
- thorough peer review by experienced researchers in your field
- rapid publication on acceptance
- support for research data, including large and complex data types
- gold Open Access which fosters wider collaboration and increased citations
- maximum visibility for your research: over 100M website views per year

At BMC, research is always in progress.

Learn more biomedcentral.com/submissions

